Primary Cosmic Ray Fluxes at Various Solar Activities

Yoshikaze SHIKAZE on behalf of the BESS Collaboration
Japan Atomic Energy Research Institute, 2-4 Shirakata-Shirane Tokai-mura, Naka-gun, Ibaraki, 319-1195, Japan

Abstract

We measured low energy cosmic-ray protons and helium nuclei observed at the small atmospheric depth through $4 - 37$ g/cm^2. These observation were carried out with BESS spectrometer launched at Lynn Lake, Manitoba, Canada from 1997 through 2002. By using realistic estimation of the atmospheric secondary protons which was tuned to reproduce BESS data at small atmospheric depths, we obtained the precise primary fluxes at the top of the atmosphere in a kinetic energy region of 0.185 – 21.5 GeV/n.

1. Introduction

Cosmic rays, charged particles from the space, enter the atmosphere at a rate of about several thousands per square meter per second. Among the cosmic-ray particles, protons and helium nuclei are dominant components, which amount about 90% and about 10% of cosmic rays, respectively. Thus the energy spectra and absolute fluxes of cosmic-ray protons and helium nuclei constitute the most fundamental data in cosmic-ray physics. The interstellar spectra carry important information on origin and propagation history of the cosmic rays in the Galaxy. Moreover, observable spectra in the heliosphere are deformed by the effect of the solar activity (solar modulation).

However, cosmic-rays observed by balloon experiment contain large amount of secondary particles produced inside the residual atmosphere. Therefore, in order to obtain the interstellar spectra and understanding of the solar modulation, precise estimation of the atmospheric effects are important.

We report here the low energy cosmic-ray proton and helium spectra measured by the BESS spectrometer for five flights in northern Canada between a period of 1997 through 2002. We also report realistic estimation of atmospheric protons which was tuned in comparison of the proton flux observed by the BESS spectrometer at small atmospheric depths.

pp. 69–80

2. Spectrometer

The BESS (Balloon-borne Experiment with a Superconducting Spectrometer) detector (Fig. 1) is a high-resolution rigidity ($R \equiv Pc/Ze$) spectrometer with a large geometrical acceptance. It was designed [1, 2] and developed [3, 4, 5, 6] as an omni-purpose spectrometer to perform precise measurement of absolute fluxes of various cosmic rays [7, 8, 9, 10], as well as highly sensitive searches for rare cosmic-ray components [11, 12, 13, 14, 15, 16]. Fig. 1 shows schematic

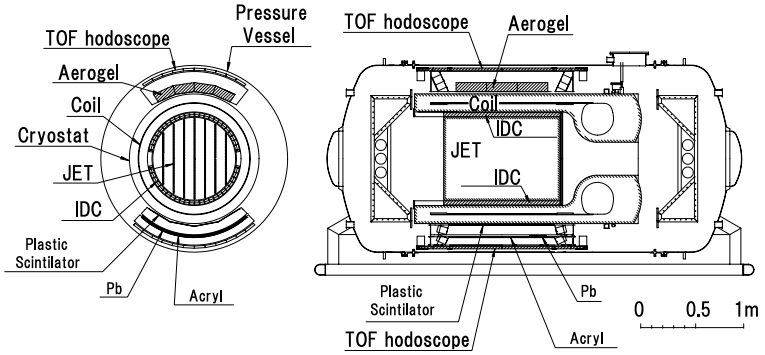

Fig 1. Cross-sectional view of the BESS detector in its 1999 configuration.

cross-sectional view of cylindrical shaped BESS rigidity spectrometer in its 1999 configuration. The large acceptance realized measurement with high statistics, and the compact and simple cylindrical structure have contribution to make systematic errors of acceptance calculation lower.

The spectrometer consists of a superconducting solenoid magnet (MAG) [2], a JET type drift chamber (JET), two inner drift chambers (IDCs), a Time-of-Flight (TOF) plastic scintillation hodoscope [6], and an aerogel Čerenkov counter [5]. A uniform magnetic field of 1 Tesla is produced by a thin superconducting coil which allows particles to pass through with small interaction probability, and the magnetic field's uniformity is a feature important for precise measurement of rigidity. The magnetic field region is filled with the central tracking detectors. Tracking of incident charged particles is performed by a circular fitting [17] up to 28 hit points in these drift chambers each with a spacial resolution of 200 μm, resulting in a magnetic-rigidity resolution of 0.5 % at 1 GV/c. This continuous, redundant, three-dimensional tracking enables recognizing background such as multi-track events and tracks having interactions or scattering. Particle identification is performed by mass measurement. The upper and lower TOF counters measure the velocity (β) and two independent ionization energy loss ($\mathrm{d}E/\mathrm{d}x$) in the scintillator. A $1/\beta$ resolution of 1.4 % was achieved in this experiment. We also measure

dE/dx in the drift chamber gas obtained as a truncated mean of the integrated charges of hit pulses. From these measurements(R, β and dE/dx) particle identification by mass is performed. Furthermore a threshold-type Čerenkov counter with silica-aerogel radiator was installed below the upper TOF hodoscopes. We selected the radiator having a refractive index of 1.02 (1.03 in 1997), in order to veto e^-/μ^- backgrounds for $\bar{p}$ up to 4.2 GeV.

For 2002 flight, we used the BESS detector developed for precise measurement of high energy protons (BESS-TeV) up to 1 TeV [18]. For this purpose, newly developed drift chambers were installed, and the detector configuration was changed as shown in Fig. 2. Fig. 2 shows the comparison of the detector configuration between the previous detector, BESS-1998 and BESS-TeV.

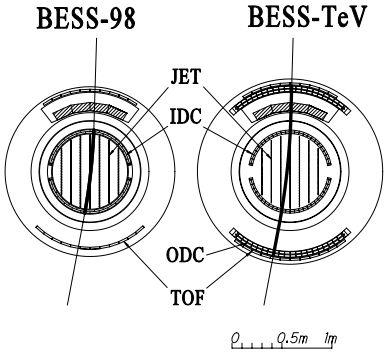

Fig 2. The detector configuration in BESS-1998 and BESS-TeV

3. Balloon Observation

The BESS scientific balloon flights were carried out from Lynn Lake ((56°5'N,101°3'W), the geomagnetic cutoff rigidity is 0.4 GV), Manitoba to near Peace River (56°2'N,117°2'W), Alberta in northern Canada in summer of 1997 1998, 1999, 2000 and 2002. The BESS spectrometer was launched from Lynn Lake, Manitoba and achieved a float altitude of 37 km, corresponding to 5 g/cm^2 of residual atmosphere. The balloon flight was terminated next evening around Peace River, Alberta, and the BESS payload came down by a parachute. It was safely recovered within a few days.

As a summary for these flights during floating level, the flight time amounts 20.5, 22.0, 34.5, 37.8 and 13.9 h., live time 18.3, 20.0, 31.3, 30.5 and 10.6 h., and recorded events 16.2, 19.0, 16.8, 15.0 and 11.3 M., in 1997, 1998, 1999, 2000 and 2002, respectively. We also obtained the data during ascending period in 1999, 2000 and 2002. As for ascending data, the flight time amounts to 2.8, 2.5 and

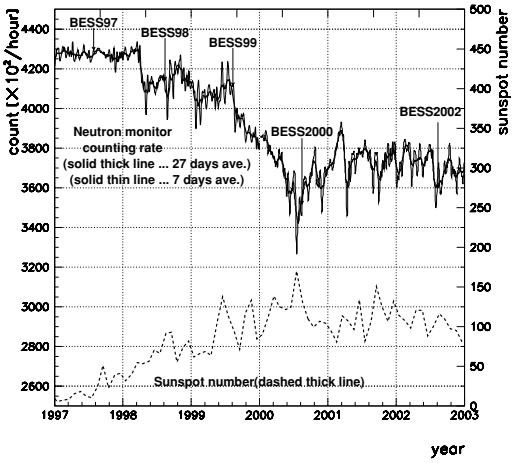

Fig 3. Counting rate of Climax neutron monitor (7 and 27 days average) and sunspot number versus year together with lines of BESS flight date.

3.9 h., live time 2.5, 2.1 and 2.7 h., and recorded events 2.3, 2.0 and 2.2 M., in 1999, 2000 and 2002, respectively.

During the duration from 1997 to 2002, solar activity have changed from the minimum to maximum phase as known from the neutron monitor [19] and the sunspot numbers as shown in Fig. 3.

4. Analysis

The procedure of data analysis and flux calculation was almost the same as that of the previous balloon flight data [7, 9, 10] except for the correction of the atmospheric effects.

Particle identification of protons is as follows. The off-line analysis selects events with a single track fully contained in the fiducial region of the tracking detectors with acceptable track qualities. Particle's charge is identified by the energy loss measurement. Both $\mathrm{d}E/\mathrm{d}x$ in upper and lower TOF scintillators must be proton-like. Moreover, particles with proton mass are selected by β-band cut. These proton selections are shown in Figure 4.

Proton fluxes at the top of the instrument(TOI) are obtained after the corrections of efficiencies such as selection, trigger and acceptance. The flux at TOI is the flux at about $5g/cm^2$, and not corrected for atmospheric effects. Proton flux at TOI consists of surviving primary component and secondary component. The secondary protons are generated from the interaction of cosmic rays with air nuclei.

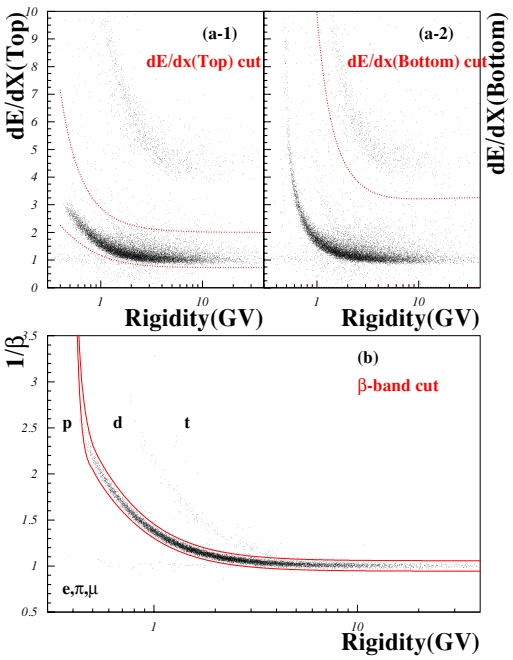

Fig 4. Proton selection by $\mathrm{d}E/\mathrm{d}x$-band cut and β-band cut

4.1. Helium nuclei

Helium nuclei were clearly identified by using both upper and lower TOF $\mathrm{d}E/\mathrm{d}x$. Since the $1/\beta$-band cut include both ^{3}He and ^{4}He, obtained helium fluxes include both ^{3}He and ^{4}He. In conformity with previous experiments, all doubly charged particles were analyzed as ^{4}He.

5. Correction of atmospheric secondary protons

In order to obtain the flux at the top of atmosphere(TOA), correction of the atmospheric effects must be estimated.

For low energy proton below 1 GeV, there are larger modulation effect and more secondary proton as the energy decreases from the estimation of secondary protons in Papini et al. [20].

5.1. Calculation tuned by observed proton fluxes at various air depths

We also obtained the ascending data of cosmic rays in 1999 and 2000 and the descending data at Ft. Sumner (cutoff rigidity is 4.2 GV), New Mexico, USA in 2001 [1]. Particularly, the BESS-2001 data enables to compare the calculation results with observed pure secondary proton in low energy region below the cutoff.

By using these data, we have improved the parameters of elementary processes in Papini et al. [20] to reproduce better the observed data at various altitudes.

We investigated possibilities for all elementary processes of secondary proton production in Papini et al. to be tuned so as to reproduce the observed proton data at small atmospheric depths. The elementary processes treated in Papini et al. consist of four production and two loss processes, and the formers are evaporation processes from target nuclei, recoil processes, cosmic-ray nucleon inelatic interactions and production from cosmic-ray helium and heavier-nuclei spallation, and the latters are loss of particles by interactions and ionization process. As a result we tuned this calculation by increasing tail of recoil proton production function in higher energy region.

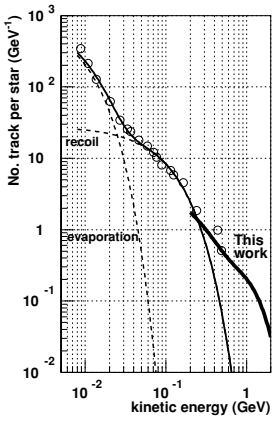

Fig 5. Recoil generation function before(dashed) and after(solid) tuning by using observed proton data in ascending and descending.

Fig. 5 shows the revised spectrum of recoil proton obtained by using BESS ascending and descending data together with the nuclear emulsion data and curves of recoil and evaporation proton spectra used in Papini et al..

Fig. 6 shows the comparison of the calculation results before and after tune with the observed data in BESS-2001. Observed proton fluxe with error bar shows cutoff effect, and protons below the cutoff energy are almost secondary component. For the calculation results corresponding to the observed proton flux, the dashed and dotted curves ((d) and (e), respectively, in Fig. 6) are drawn as that from Papini's method and that tuned in this work, respectively. The slight difference of the geomagnetic cutoff rigidity depending on the location of observation was considered to primary proton flux as input. We should mention

here that we confirmed that this calculation by Papini's mothod gave almost the same results in Papini et al. when the same primary fluxes in Papini et al. were used as input fluxes. Tuned results in this work well agree with the observed proton spectra though the calculations using original method in Papini et al. have large difference from observed proton fluxes. Both curves, (d) and (e) are the flux as primary plus secondary components, and the separated components are drawn by the solid curves, (a) for same primary component, (b) for secondary component by Papini's method and (c) for secondary conpoment in this work. The difference in both calculation methods comes from the difference of the secondary proton production process as recoil protons.

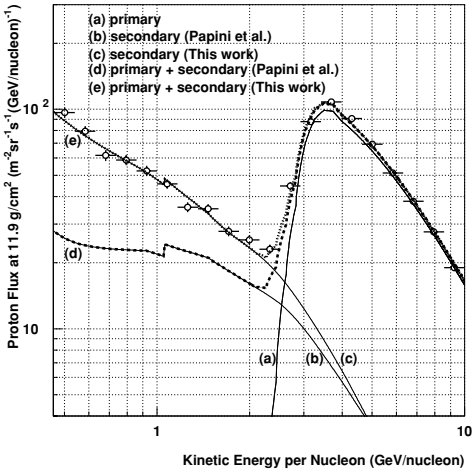

Fig 6. Comparison of calculation results of primary and secondary proton components with observed data in BESS-2001 at 11.9 g/cm^2

Since proton flux in BESS-2001 are only published above 0.46 GeV/n, we have checked the tuned calculation by comparing with proton flux observed during ascending period in BESS-2000 for more lower energy. During the ascent, special trigger mode effective for low energy proton below 1 GeV was adopted, and low energy proton data was effectively collected in spite of short ascent period. Fig. 7 shows the comparison of calculation results with observed proton data during ascending period in BESS-2000 as a function of atmospheric depth. Kinetic energy range of these observed proton fluxes are from 0.29 to 0.34, from 0.46 to 0.54 and from 0.63 to 0.73 GeV/n, while the calculated curves to be compared are for 0.32, 0.50 and 0.68 GeV/n, respectively, which are set as mean value of the range in log scale. In the analysis, zenith angle θ must satisfy $\cos\theta > 0.95$ to select protons which incident almost vertically. The thick dashed and thin dotted curves express

the calculation results obtained by Papini's method and those tuned in this work, respectively. These calculations start from averaged floating level using the flux obtained during floating period. The incident angle dependence of the initial input spectra at start depth is obtained by the calculation starting from the top of the atmosphere. As shown in Fig. 7, tuned results well flows the growth curves of proton flux at low energy region. This is the check by using the flux as primary plus secondary components though the check of low energy region below the cutoff rigidity using BESS-2001 data was made by using only secondary component.

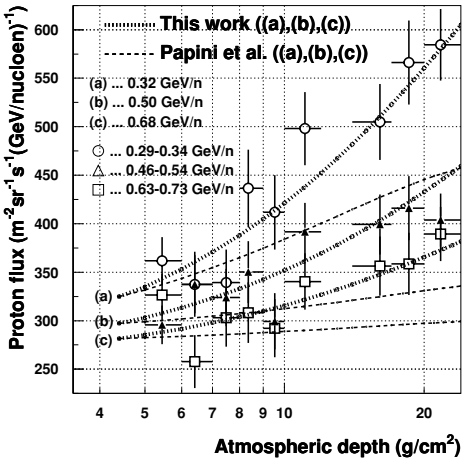

Fig 7. Comparison of calculations with fluxes observed during ascending period in BESS-2000 as a function of atmospheric depth.

6. Results and Discussions

6.1. Proton and Helium fluxes at the top of the atmosphere(TOA)

Thus, as for the correction of the atmospheric effects, we used more realistic calculation to estimate the atmospheric secondary proton fluxes at any solar activity from 1997 to 2002, and proton fluxes at TOA are obtained. In Fig. 8, large solar modulation effect are shown in the proton flux in 2000. Sudden decrease of proton flux from 1999 to 2000 was observed.

In the same way, helium spectra were obtained. Fig. 8 also shows helium fluxes at TOA from 1997 to 2000. It should be noted that helium fluxes are plotted after being divided by 10. Large solar modulation effect and sudden decrease are also shown in the helium flux in 2000.

Both proton and helium fluxes in 2002 have slightly increased from those in 2000, and this time variation from 2000 to 2002 is smaller than the variation from 1999 to 2000 around the solar magnetic field reversal.

It should be noticed that this analysis is different from previous data for BESS-1998 by the different atmospheric collection, and that the atmospheric collection is different from previous data for BESS-1999 and -2000 since the recoil tunning for more precise estimation of secondary proton production has improved by using pure secondary proton data below the cutoff rigidity observed during BESS-2001 descending period.

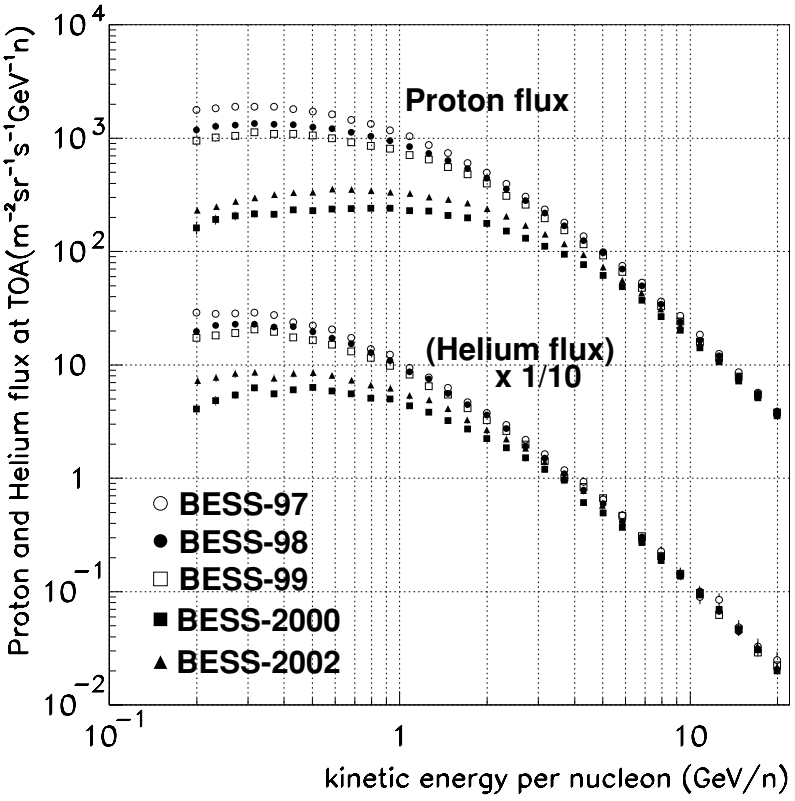

Fig 8. Proton and helium fluxes at TOA from 1997 to 2002

6.2. Force Field Approximation

Taking the value of "modulation parameter" ϕ at the flight date, we can estimate the interstellar (IS) proton flux by assuming the Force Field approxima-

tion [21]. The approximation for the proton flux is clearly seen in Fig. 9, where IS proton flux is determined by assuming ϕ ∼600 MV for BESS-1998 (estimated in Myers et al. [22]) and to be described by : $A\beta^{P_1}R^{-P_2}$, where β is the particle to the light velocity ratio, R is the rigidity, A, P_1 and P_2 are the fitting parameters (The results are noted in Fig. 9. The P_2, power of R depends on the assumption of ϕ.). Other curves and the value of ϕ noted in Fig. 9 are obtained by fitting the BESS data using the approximation and the IS proton flux.

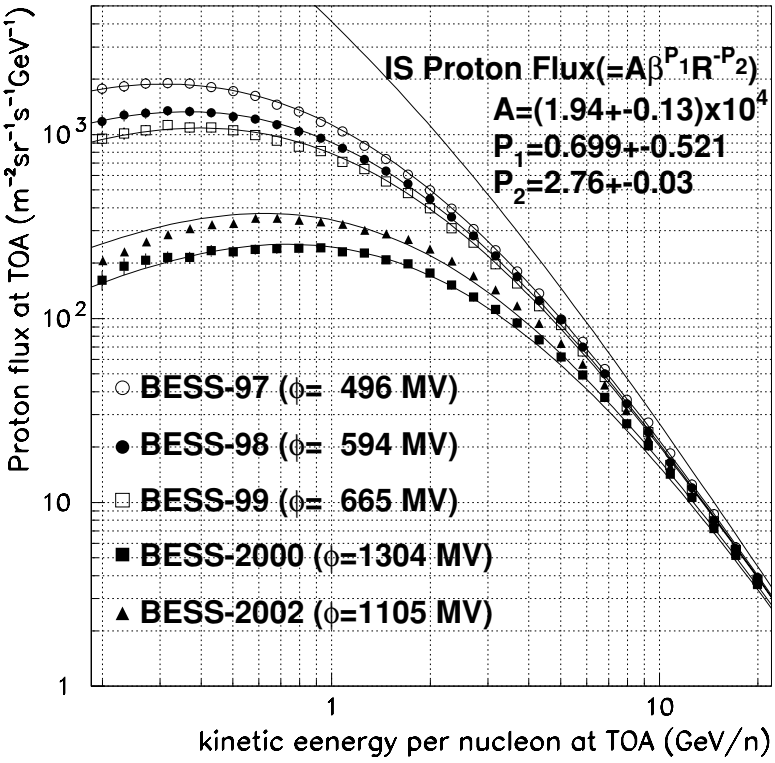

Fig 9. Force Field approximation for protons. The interstellar (IS) proton flux is determined by assuming ϕ∼600 MV for BESS-1998. Other curves and the value of ϕ are obtained by fitting the BESS data using the approximation and the IS proton flux.

The value of χ^2 for the fitting in Fig. 9 are 3.17, 4.25, 6.18, 24.6 and 55.6 , for 1997, 1998, 1999, 2000 and 2002, respectively. Fig. 10 shows the χ^2 using data points in fitting range as a function of lower limit of kinetic energy per nucleon in fitting to obtain the modulation parameter, ϕ, respectively. In all case in Fig. 10,

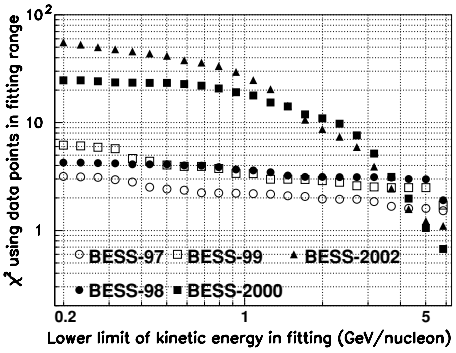

Fig 10. The χ^2 versus lower limit of kinetic energy per nucleon in fitting for χ^2 calculation using data points in fitting range. Upper limit is fixed at 20 GeV/n.

upper limit is fixed at 20 GeV/n.

The results for 2000 and 2002 show different tendency from others, which depends on the range to apply. Though the results for 1997, 1998 and 1999 in Fig. 9 and 10 show that the Force Field approximation follows the time variation of proton flux well up to low energy of 0.2 GeV/n, while the large modulation effect in 2000 and 2002 is difficult to be described by the simple approximation with single ϕ for the same energy region.

7. Conclusion

Low energy cosmic-ray proton and helium spectra have been measured during the BESS balloon flights in northern Canada from solar minimum through post-maximum. Their fluxes at TOA for five flights were obtained by using the calculation of atmospheric protons revised to agree with the secondary protons observed during descending period at Ft. Sumner and ascending period at Lynn Lake (cutoff rigidity is 4.2 and 0.4 GV, respectively). From the results of analysis, sudden decrease of the low energy fluxes in 2000 was observed at the solar polarity reversal. Charge dependent solar modulation model in Bieber et al. well follows the time variation of proton intensity observed by BESS at the solar polarity reversal between 1999 and 2000. The fitting result of our proton spectra by the Force Field approximation indicates that the flux deformation from the fitted lines by the large modulation effect in 2000 solar maximum and in 2002 are larger than those from 1997 solar minimum to 1999 which are described comparatively better by the the approximation.

References

[1] S. Orito, in: Proceedings of ASTROMAG Workshop, KEK Report KEK87-19 (1987) 111.
[2] A. Yamamoto, et al., IEEE Trans. Magn. 24 (1988) 1421.
[3] A. Yamamoto, et al., Adv. Space Res. 14 (1994) 75.
[4] Y. Ajima, et al., Nucl. Instrum. Methods A 443 (2000) 71.
[5] Y. Asaoka, et al., Nucl. Instrum. Methods A 416 (1998) 236.
[6] Y. Shikaze, et al., Nucl. Instrum. Methods A 455 (2000) 596.
[7] T. Sanuki, et al., Astrophys. J. 545 (2000) 1135.
[8] M. Motoki, et al., Astropart. Phys. 19 (2003) 113.
[9] K. Abe, et al., Phys. Lett. B 564 (2003) 8.
[10] T. Sanuki, et al., Phys. Lett. B 577 (2003) 10.
[11] K. Yoshimura, et al., Phys. Rev. Lett. 75 (1995) 3792; A. Moiseev, et al., Astrophys. J. 474 (1997) 479.
[12] H. Matsunaga, et al., Phys. Rev. Lett. 81 (1998) 4052.
[13] S. Orito, et al., Phys. Rev. Lett. 84 (2000) 1078.
[14] T. Maeno, et al., Astropart. Phys. 16 (2001) 121.
[15] Y. Asaoka, et al., Phys. Rev. Lett. 88 (2002) 051101.
[16] M. Sasaki, et al., Nucl. Phys. B (Proc. Suppl.) 113 (2002) 202.
[17] V. Karimaki, Comput. Phys. Commun. 69 (1992) 133.
[18] S. Haino, et al., Nucl. Instrum. Methods A 518 (2004) 167.
[19] http://odysseus.uchicago.edu/NeutronMonitor/: University of Chicago, "National Science Foundation Grant ATM-9613963".
[20] P. Papini, et al., Nuovo Cimento 19C (1996) 367.
[21] L.J. Gleeson, W.I. Axford, Astrophys. J. 154 (1968) 1101.
[22] Z.D. Myers, E.S. Seo, Adv. Space Res. (2002) (submitted).